The Generalized Singular Value Decomposition and the Method of Particular Solutions

Betcke, Timo

2007

MIMS EPrint: **2006.396**

Manchester Institute for Mathematical Sciences
School of Mathematics

The University of Manchester

Reports available from: http://eprints.maths.manchester.ac.uk/
And by contacting: The MIMS Secretary
School of Mathematics
The University of Manchester
Manchester, M13 9PL, UK

ISSN 1749-9097

THE GENERALIZED SINGULAR VALUE DECOMPOSITION AND THE METHOD OF PARTICULAR SOLUTIONS

TIMO BETCKE*

Abstract. A powerful method for solving planar eigenvalue problems is the Method of Particular Solutions (MPS), which is also well known under the name "point matching method". The implementation of this method usually depends on the solution of one of three types of linear algebra problems: singular value decomposition, generalized eigenvalue decomposition, or generalized singular value decomposition. We compare and give geometric interpretations of these different variants of the MPS. It turns out that the most stable and accurate of them is based on the Generalized Singular Value Decomposition. We present results to this effect and demonstrate the behavior of the generalized singular value decomposition in the presence of a highly ill-conditioned basis of particular solutions.

Key words. eigenvalues, method of particular solutions, point matching, subspace angles, generalized singular value decomposition

AMS subject classifications. 65F15, 65F22, 65N25

1. Introduction. The idea of the Method of Particular Solutions is to approximate eigenvalues and eigenfunctions of

$$-\Delta u = \lambda u \quad \text{in } \Omega \tag{1.1a}$$

$$u = 0 \quad \text{on } \partial\Omega, \tag{1.1b}$$

from a space of particular solutions that satisfy (1.1a) but not necessarily (1.1b). In this article we assume that Ω is a planar region.

A famous article on this method was published in 1967 by Fox, Henrici and Moler [17] who used the MPS to compute the smallest eigenvalues of the L-shaped region to up to 8 digits of accuracy. Very similar ideas were also contained in the earlier papers by Conway et. al. [10, 11]. The MPS is also known under the name "point matching method" in the literature (see for example [10]). Closely related is also the Method of Fundamental Solutions [9, 23]. The results of this paper apply equally well to the application of these methods to elliptic eigenvalue problems.

The MPS is especially effective for very accurate computations. Although mesh-based methods like FEM can be tuned to deliver exponential convergence on certain regions (e.g. *hp*-FEM methods) the implementation can be a difficult task while the MPS can often be implemented in a few lines of Matlab code (see for example the Matlab code given in [7]). Also the computation of eigenvalues with very large wave numbers seems to be very suitable for the MPS. While the matrix sizes in FEM based methods grow rapidly for high eigenvalues the computational effort of the MPS still stays reasonable, especially if accelerated variants like the "scaling method" are used [1].

Unfortunately, the MPS suffers from problems for complicated regions coming from ill-conditioning of the basis functions. These problems were observed in the paper of Fox, Henrici and Moler and also noted by later authors (see for example [13]). In [7] we returned to the original idea of the MPS and showed that the reformulation of the MPS as a problem of computing the angle between certain subspaces makes

*School of Mathematics, The University of Manchester, Oxford Road, Manchester, M13 9PL, UK `timo.betcke@maths.man.ac.uk`.

it applicable to a variety of polygonal and other planar regions. Numerical examples show that even for complicated regions eigenvalues can be computed to 10 digits or more with this subspace angle approach.

While writing [7] we were not aware that independently of the numerical analysis community, physicists had developed very similar methods in connection with semi-classical mechanics and quantum chaos. This fact was brought to our attention in 2004 by Barnett. The physicists are particularly interested in eigenmodes related to high wave numbers. One of the leaders of this effort has been Heller, who together with his colleagues has developed methods closely related to the MPS [19, 20], though using different terminology. Another key contribution in this area was the "scaling method" of Vergini and Saraceno. These ideas were recently brought together and improved in Barnett's thesis [1].

In this paper we review the various methods of particular solutions and show that a suitable tool to describe them is the generalized singular value decomposition. From the various linear algebra tools which are used in the different methods, i.e. the singular value decomposition (SVD), the generalized eigenvalue decomposition (GEVD) and the generalized singular value decomposition (GSVD), it turns out that the GSVD leads to the most robust and widely applicable approach. Furthermore, it turns out that the subspace angle method proposed in [7] is just a GSVD in disguise. Hence, the stability results which we discuss in this paper are also valid for the subspace angle method and lead to a further understanding of this method.

The paper is organized as follows. In Section 2 we present the Method of Particular Solutions (MPS) and its implementations using the SVD, GEVD and GSVD.

While singular values are perfectly conditioned this is not true for generalized singular values. Therefore, in Section 3 we investigate the numerical stability of the GSVD approach. In Section 4 we analyze a regularization strategy for the GSVD, which was proposed by Barnett for the GEVD approach to the MPS.

In Section 5 we discuss the limits of the GSVD if the basis of particular solutions only admits ill-conditioned representations of approximate eigenfunctions. The paper finishes in Section 6 with a short summary and conclusions.

All notation is standard. We will frequently use ϵ_{mach} for the machine precision ($\epsilon_{mach} \approx 2.2 \times 10^{-16}$ in IEEE arithmetic).

2. The Method of Particular Solutions. The Method of Particular Solutions (MPS) approximates eigenpairs (λ_k, u_k) of (1.1) from a space of functions that satisfy (1.1a), but not necessarily (1.1b). Let

$$\mathcal{A}(\lambda) := \operatorname{span}\{\Phi_1(\lambda; z), \ldots, \Phi_p(\lambda; z)\} \subset \mathcal{C}^2(\Omega) \cap \mathcal{C}(\overline{\Omega}) \tag{2.1}$$

be such a space. Therefore,

$$-\Delta\Phi_k(\lambda; z) = \lambda\Phi_k(\lambda; z), \;\; k = 1, \ldots, p$$

for $z \in \Omega$. Fox, Henrici and Moler used Fourier-Bessel functions of the form $\Phi_k(\lambda; z) = J_{\alpha k}(\sqrt{\lambda}r)\sin(\alpha k\theta)$ that are the exact solutions of (1.1) in a wedge with interior angle π/α. In physics frequently real plane waves and evanescent plane waves are used as particular solutions [5]. Other possible sets of basis functions are fundamental solutions which solve the eigenvalue equation (1.1a) in Ω but have singularities located outside of $\overline{\Omega}$ [15].

To make the notation easier we will from now on always write $\Phi_k(z)$ instead of $\Phi_k(\lambda; z)$ since the dependence of the particular solutions on λ will be clear from the context.

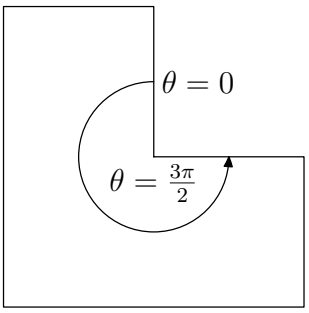

FIG. 2.1. *The L-shaped region.*

2.1. An SVD based formulation of the MPS. Let $z_1, \ldots, z_n \in \partial\Omega$ be boundary collocation points. We are looking for a value λ for which there exists a linear combination

$$\Phi = \sum_{k=1}^{p} c_k \Phi_k$$

of basis functions which is small at these points. This is then hopefully a good approximation to an eigenfunction of (1.1). Let $A_B(\lambda)$ be the matrix of basis functions evaluated at the z_k, i.e. $(A_B(\lambda))_{jk} = \Phi_k(z_j)$, $j = 1, \ldots, n$, $k = 1, \ldots, p$. The method is then formulated as the following minimization problem.

$$\min_{\lambda} \min_{c \in \mathbb{R}^p \setminus \{0\}} \frac{\|A_B(\lambda)c\|_2}{\|c\|_2} = \min_{\lambda} \xi_p(\lambda), \tag{2.2}$$

where $\xi_p(\lambda)$ is the smallest singular value of the matrix $A_B(\lambda)$.

The formulation (2.2) is due to Moler [24]. In earler approaches the number of collocation points n was chosen identically to the number of basis functions p. In that case $A_B(\lambda)$ is square and λ was determined by solving

$$\det(A_B(\lambda)) = 0$$

(see for example [17]).

The SVD approach can fail if $A_B(\lambda)$ is ill-conditioned for some $\lambda > 0$ far from an eigenvalue. Assume that λ is not close to an eigenvalue and that $A_B(\lambda)$ is ill-conditioned. Then there exists a vector $c \in \mathbb{R}^p$ with $\|c\|_2 = 1$ such that $\|A_B(\lambda)c\|_2 \ll 1$. But the unique solution of (1.1) if λ is not an eigenvalue is the zero function. Hence, the function defined by the coefficent vector c will approximate this zero function. In [7] these functions are called "spurious solutions" of (1.1).

In Figure 2.2 we demonstrate this failure for the example of the L-shaped region from Figure 2.1. The upper left plot shows the curve $\xi_p(\lambda)$ for $p = 10$ Fourier-Bessel basis functions of the form $\Phi_k(r, \theta) = J_{\frac{2k}{3}}(\sqrt{\lambda}r) \sin \frac{2k}{3}\theta$. The origin of the polar coordinates is at the reentrant corner with the line $\theta = 0$ directed as in Figure 2.1. The minima of $\xi_p(\lambda)$ in the upper left plot of Figure 2.2 point to the first three eigenvalues of (1.1) on this region. In the lower left plot we have chosen $p = 60$. Now the minima at the eigenvalues are not visible any more on this plotting scale since $\xi_p(\lambda)$ is small also away from the eigenvalues.

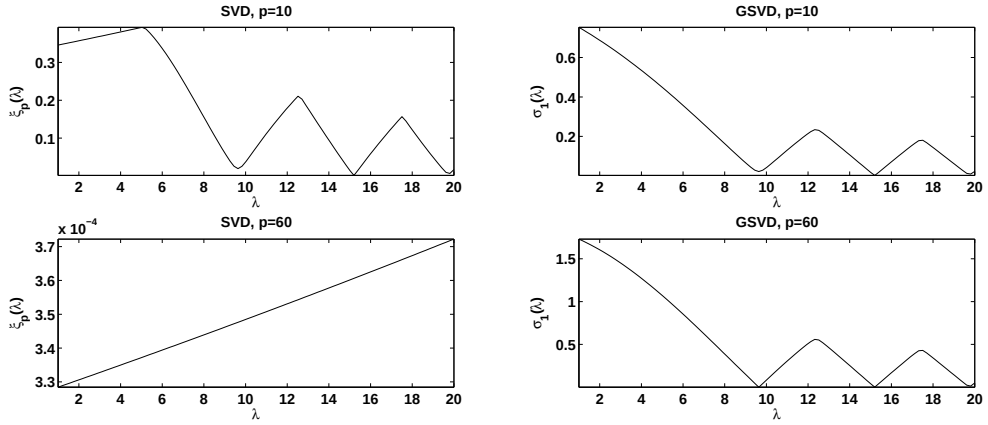

FIG. 2.2. *Comparison of the SVD and GSVD approach on the L-shaped region for $p = 10$ and $p = 60$ basis functions.*

The cure is to choose basis functions that are approximately orthogonal in Ω. Such bases were analytically constructed for some regions by Moler in [24]. An automatic way to obtain bases that are approximately orthogonal in the interior of the region is delivered by the GSVD.

2.2. A GSVD formulation. We want to cure the problem of ill-conditioned bases in the SVD approach by orthogonalizing the basis functions in the interior of Ω. Let $\bar{z}_1, \ldots, \bar{z}_m \in \Omega$ be a set of interior points and let $A_I(\lambda)$ be the matrix of basis functions evaluated at these interior points, i.e. $(A_I(\lambda))_{jk} = \Phi_k(\bar{z}_j)$, $j = 1, \ldots, m$, $k = 1, \ldots, p$. For the moment assume that $m \geq p$ and that $A_I(\lambda)$ has full column rank. Let

$$A_I(\lambda) = Q(\lambda)R(\lambda)$$

be the QR decomposition of $A_I(\lambda)$. Instead of the discrete basis set given by the columns of $\begin{bmatrix} A_B(\lambda) \\ A_I(\lambda) \end{bmatrix}$ we use

$$\begin{bmatrix} A_B(\lambda) \\ A_I(\lambda) \end{bmatrix} R(\lambda)^{-1} = \begin{bmatrix} A_B(\lambda)R(\lambda)^{-1} \\ Q(\lambda) \end{bmatrix},$$

in the SVD approach. This is equivalent to orthogonalizing the particular solutions in a discrete inner product over the interior discretization points. We obtain

$$\sigma_1(\lambda) := \min_{y \in \mathbb{R}^p \setminus \{0\}} \frac{\|A_B(\lambda)R(\lambda)^{-1}y\|_2}{\|y\|_2}$$

This approach guarantees that every coefficient vector y with $\|y\|_2 = 1$ leads to a trial function that is of unit discrete norm over the interior points $\bar{z}_1, \ldots, \bar{z}_m$. We therefore avoid spurious solutions that are nearly zero in the interior of the region.

For $y = R(\lambda)x$ it follows that

$$\sigma_1(\lambda) = \min_{y \in \mathbb{R}^p \setminus \{0\}} \frac{\|A_B(\lambda)R(\lambda)^{-1}y\|_2}{\|y\|_2} = \min_{x \in \mathbb{R}^p \setminus \{0\}} \frac{\|A_B(\lambda)x\|_2}{\|A_I(\lambda)x\|_2}.$$

We can reformulate the last equation as the generalized eigenvalue problem

$$A_B(\lambda)^T A_B(\lambda) x(\lambda) = \sigma_1(\lambda)^2 A_I(\lambda)^T A_I(\lambda) x(\lambda),$$

where the value $\sigma_1(\lambda)^2$ is the smallest eigenvalue of the pencil $\{A_B(\lambda)^T A_B(\lambda), A_I(\lambda)^T A_I(\lambda)\}$. However, by using the GSVD we can compute the value $\sigma_1(\lambda)$ directly without using the squared matrices $A_B(\lambda)^T A_B(\lambda)$ and $A_I(\lambda)^T A_I(\lambda)$. The definition of the GSVD in the following Theorem is a simplified version of the definition given by Paige and Saunders in [25].

THEOREM 2.1 (Generalized Singular Value Decomposition). *Let $A \in \mathbb{R}^{n\times p}$ and $B \in \mathbb{R}^{m\times p}$ be given with $n \geq p$. Define $Y = \begin{bmatrix} A \\ B \end{bmatrix}$ and assume that $rank(Y) = p$. There exist orthogonal matrices $U \in \mathbb{R}^{n\times n}$ and $W \in \mathbb{R}^{m\times m}$ and a nonsingular matrix $X \in \mathbb{R}^{p\times p}$ such that*

$$A = USX^{-1}, \quad B = WCX^{-1},$$

where $S \in \mathbb{R}^{n\times p}$ and $C \in \mathbb{R}^{m\times p}$ are diagonal matrices defined as $S = diag(s_1, \ldots, s_p)$ and $C = diag(c_1, \ldots, c_{\min\{m,p\}})$ with $0 \leq s_1 \leq \cdots \leq s_p \leq 1$ and $1 \geq c_1 \geq \cdots \geq c_{\min\{m,p\}} \geq 0$. Furthermore, it holds that $s_j^2 + c_j^2 = 1$ for $j = 1, \ldots, \min\{m, p\}$ and $s_j = 1$ for $j = m+1, \ldots, p$.

If $m < p$ we define

$$c_{m+1} = \cdots = c_p = 0. \tag{2.3}$$

Then $s_j^2 + c_j^2 = 1$ for all $j = 1, \ldots, p$. The values $\sigma_j = s_j/c_j$ are called the generalized singular values of the pencil $\{A, B\}$. If $c_j = 0$ then $\sigma_j = \infty$. The jth column x_j of X is the right generalized singular vector associated with σ_j.

From Theorem 2.1 it follows that

$$c_j^2 A^T A x_j = s_j^2 B^T B x_j.$$

Hence, the finite generalized singular values are the square roots of the finite generalized eigenvalues of the pencil $\{A^T A, B^T B\}$. But as in the case of the standard SVD they can be computed without using this squared formulation. In Matlab this is implemented by the `gsvd` function.

Similarly to singular values the finite generalized singular values of a pencil $\{A, B\}$ have a minimax characterization as

$$\sigma_j = \min_{\substack{H \subset \mathbb{R}^p \\ dim(H)=j}} \max_{\substack{x \in H \\ Bx \neq 0}} \frac{\|Ax\|_2}{\|Bx\|_2}. \tag{2.4}$$

This minimax characterization is an immediate consequence of the minimax characterization of singular values. A short proof is for example contained in [8, Thm. 3.4.2].

It follows that the value $\sigma_1(\lambda)$ is the smallest generalized singular value of the pencil $\{A_B(\lambda), A_I(\lambda)\}$. Approximations to the eigenvalues of (1.1) are then given by the minima of $\sigma_1(\lambda)$ in dependence on λ. Note that the GSVD does not require $m \geq p$ for $A_I(\lambda)$.

In the two right plots of Figure 2.2 we show the smallest generalized singular value $\sigma_1(\lambda)$ for different values of λ on the L-shaped region. While for $p = 10$ basis

functions it is similar to the curve computed by the SVD approach we see a large difference for $p = 60$ basis functions. As explained earlier the SVD fails here but the GSVD still lets us easily spot the three minima that point to the eigenvalues.

The application of the GSVD to the MPS was also considered in unpublished work by Eisenstat.[1] His motivation was the minimization of error bounds for the MPS. In the physics community a related approach was introduced by Heller under the name Plane Wave Decomposition Method (PWDM) [19, 20]. He used only one point in the interior of the region to normalize the approximate eigenfunctions. A discussion of this method is contained in [1]. In the engineering literature the GSVD has been used in a related context to regularize boundary element formulations for the Laplace eigenvalue problem [22].

The GSVD has an interesting interpretation in terms of angles between subspaces. The smallest principal angle θ_1 between two spaces $\mathcal{S}_1 \subset \mathbb{R}^n$ and $\mathcal{S}_2 \subset R^n$ is defined by

$$\cos\theta_1 = \max_{\substack{x\in\mathcal{S}_1,\ \|x\|_2=1\\ y\in\mathcal{S}_2,\ \|y\|_2=1}} \langle x, y\rangle.$$

THEOREM 2.2. *Define $\mathcal{D}_0 \subset R^{n+m}$ as the space of vectors whose first n entries are zero. Denote by $\mathcal{A}(\lambda)$ the span of the columns of $A(\lambda) := \begin{bmatrix} A_B(\lambda) \\ A_I(\lambda)\end{bmatrix}$. Let $\theta_1(\lambda)$ be the smallest principal angle between $\mathcal{D}_0$ and $\mathcal{A}(\lambda)$. Then $\tan\theta_1(\lambda) = \sigma_1(\lambda)$, where $\sigma_1(\lambda)$ is the smallest generalized singular value of the pencil $\{A_B(\lambda), A_I(\lambda)\}$.*

Proof. Let $D_0 := \begin{bmatrix} 0 \\ I\end{bmatrix} \in \mathbb{R}^{(n+m)\times m}$. Then

$$\begin{aligned}\cos\theta_1(\lambda) &= \max_{\substack{x\in\mathbb{R}^m,\\ y\in\mathbb{R}^p}} \frac{\langle D_0 x, A(\lambda)y\rangle}{\|D_0 x\|_2\|A(\lambda)y\|_2} = \max_{\substack{x\in\mathbb{R}^m,\\ y\in\mathbb{R}^p}} \frac{x^T A_I(\lambda)y}{\|x\|_2\|A(\lambda)y\|_2}\\ &= \max_{y\in\mathbb{R}^p} \frac{\|A_I(\lambda)y\|_2}{\sqrt{\|A_B(\lambda)y\|_2^2 + \|A_I(\lambda)y\|_2^2}},\end{aligned}$$

from which it follows that

$$\tan\theta_1(\lambda) = \min_{y\in\mathbb{R}^p} \frac{\|A_B(\lambda)y\|_2}{\|A_I(\lambda)y\|_2} = \sigma_1(\lambda).$$

□ We can therefore interpret the GSVD approach in a different way. We want to minimize the angle $\theta_1(\lambda)$ between the space of functions that are zero on the boundary collocation points and the space of particular solutions evaluated on boundary and interior points. Based on this idea the subspace angle method was introduced in [7]. Theorem 2.2 shows that this idea is completely equivalent to the GSVD approach. Indeed, let $(c_1(\lambda), s_1(\lambda))$ be the generalized singular value pair associated with $\sigma_1(\lambda)$, that is $\sigma_1(\lambda) = s_1(\lambda)/c_1(\lambda)$ and $s_1(\lambda)^2 + c_1(\lambda)^2 = 1$. Then the subspace angle method from [7] computes the value $s_1(\lambda)$.

2.3. Comparison to generalized eigenvalue formulations. Based on the minimization of error bounds for the Method of Particular Solutions Kuttler and Sigillito [21] published in 1978 a formulation of the MPS which uses the GEVD.

[1] He used it to compute the first eigenvalues of the C-shaped region on the occasion of Cleve Moler's 60th birthday in 1999.

(Eisenstat remarked that this idea even goes back to Bergman in 1936 [4].) This was independently rediscovered by Heller's student Barnett [1].

Let the minimal error on the boundary within the space $\mathcal{A}(\lambda)$ be defined as

$$t_m(\lambda) = \min_{\Phi \in \mathcal{A}(\lambda)\setminus\{0\}} \frac{\|\Phi\|_{\partial\Omega}}{\|\Phi\|_{\Omega}}, \tag{2.5}$$

where

$$\begin{aligned} \|\Phi\|_{\partial\Omega} &:= \left(\int_{\partial\Omega} \Phi(s)^2 ds\right)^{\frac{1}{2}} = \langle \Phi, \Phi\rangle_{\partial\Omega}^{\frac{1}{2}} \\ \|\Phi\|_{\Omega} &:= \left(\int_{\Omega} \Phi(x,y)^2 dxdy\right)^{\frac{1}{2}} = \langle \Phi, \Phi\rangle_{\Omega}^{\frac{1}{2}} \end{aligned} \tag{2.6}$$

are the L^2-norms of u on the boundary $\partial\Omega$ and in the interior of Ω and $\langle\cdot,\cdot\rangle_{\partial\Omega}$ and $\langle\cdot,\cdot\rangle_{\Omega}$ are the associated inner products. If $t_m(\lambda) = 0$ then λ is an eigenvalue. Usually we won't be able to exactly represent an eigenfunction as a linear combination of functions in $\mathcal{A}(\lambda)$. Therefore, we are looking for the minima of $t_m(\lambda)$. These are then approximations to the eigenvalues of (1.1). This strategy was also proposed by Eisenstat in [14].

$t_m(\lambda)$ can be expressed as

$$t_m(\lambda)^2 = \min_{\Phi \in \mathcal{A}(\lambda)\setminus\{0\}} \frac{\|\Phi\|_{\partial\Omega}^2}{\|\Phi\|_{\Omega}^2} = \min_{x \in \mathbb{R}^p\setminus\{0\}} \frac{x^T F(\lambda) x}{x^T G(\lambda) x},$$

where $(F(\lambda))_{jk} := \langle \Phi_j, \Phi_k\rangle_{\partial\Omega}$ and $(G(\lambda))_{jk} := \langle \Phi_j, \Phi_k\rangle_{\Omega}$. Hence, the value $t_m(\lambda)^2$ is just the smallest eigenvalue $\mu_1(\lambda)$ of the generalized eigenvalue problem

$$F(\lambda)x(\lambda) = \mu(\lambda) G(\lambda) x(\lambda). \tag{2.7}$$

Barnett used this formulation to compute eigenvalues on the stadium billiard to several digits of accuracy [1].

In praxis the integrals appearing in this method are usually evaluated by quadrature rules of the form

$$\int_{\partial\Omega} \Phi(s)^2 ds \approx \sum_{j=1}^{n} w_j^B \Phi^2(z_j), \quad \text{and} \quad \int_{\Omega} \Phi(s)^2 ds \approx \sum_{j=1}^{m} w_j^I \Phi^2(\tilde{z}_j)$$

with positive weights w_j^B and w_j^I. Let

$$W_B = \operatorname{diag}(w_1^B, \ldots, w_n^B) \quad \text{and} \quad W_I = \operatorname{diag}(w_1^I, \ldots, w_n^I). \tag{2.8}$$

Then

$$\bar{F}(\lambda) = A_B(\lambda)^T W_B A_B(\lambda), \quad \bar{G}(\lambda) = A_I(\lambda)^T W_I A_I(\lambda) \tag{2.9}$$

are the matrices obtained by the quadrature rules. For the smallest eigenvalue $\bar{\mu}_1(\lambda)$ of the pencil $\{\bar{F}, \bar{G}\}$ we have $t_m(\lambda) \approx \bar{\mu}_1(\lambda)^{1/2}$. However, the structure of the pencil $\{\bar{F}, \bar{G}\}$ allows the application of the GSVD to directly compute an approximation of $t_m(\lambda)$, namely for the smallest generalized singular value $\bar{\sigma}_1(\lambda)$ of the pencil $\{W_B^{\frac{1}{2}} A_B(\lambda), W_I^{\frac{1}{2}} A_I(\lambda)\}$ we have $\bar{\sigma}_1(\lambda) = \bar{\mu}_1(\lambda)^{1/2} \approx t_m(\lambda)$. The only difference to

the formulation in Section 2.2 are the matrices $W_B^{1/2}$ and $W_I^{1/2}$ from the quadrature rules. But it is not important to choose a very accurate quadrature rule. Numerical experiments suggest that we just need a sufficient number of boundary points to sample the trial functions on $\partial\Omega$ and sufficiently many random interior points to ensure that we do not get spurious solutions that are almost zero in the interior of Ω [7].

While we compute with the GSVD directly an approximation for $t_m(\lambda)$ we compute with the GEVD an approximation for $t_m(\lambda)^2$, which can limit the attainable accuracy in computing the minima of $t_m(\lambda)$ as we demonstrate now. In [2] Barnett showed that around an eigenvalue λ_k the function $\mu_1(\lambda)$ behaves quadratically. We can therefore model it there as $\mu_1(\lambda) \approx \mu_1(\lambda_k) + C(\lambda - \lambda_k)^2$ for some $C > 0$. Computing the eigenvalues of $\{\bar{F}(\lambda), \bar{G}(\lambda)\}$ by a standard solver like Matlab's `eig` can produce absolute errors at least in the order of machine precision. In an interval around λ_k with width $2\sqrt{\epsilon_{mach}/C}$ these are of the same magnitude or larger than $|\mu_1(\lambda) - \mu_1(\lambda_k)|$ due to the quadratic behaviour of $\mu_1(\lambda)$ there. Hence, in this interval of size $\Theta(\sqrt{\epsilon_{mach}})$ we may not be able to detect the minimum of $t_m(\lambda)$.

If we directly compute the smallest generalized singular value $\sigma_1(\lambda)$ of the pencil $\{A_B(\lambda), A_I(\lambda)\}$ by a standard GSVD solver like `gsvd` in Matlab we can expect errors in the computed value $\tilde{\sigma}_1(\lambda)$ in the order of machine precision if the problem is well-conditioned. Since $\sigma_1(\lambda)$ is almost linear close to λ_k the floating point errors are only of the same magnitude or larger than $|\sigma_1(\lambda) - \sigma_1(\lambda_k)|$ in an interval around λ_k with width $\Theta(\epsilon_{mach})$. Hence, we expect to find the minima of $\sigma_1(\lambda)$ to an accuracy of almost machine precision.

In Figure 2.3 we demonstrate this for the example of the L-shaped region from Figure 2.1. From now on we plot only the computed points rather than connected lines to better emphasize numerical errors in the plotted curves. We approximate $\mu_1(\lambda)$ by the smallest eigenvalue of the pencil $\{A_B(\lambda)^T A_B(\lambda), A_I(\lambda)^T A_I(\lambda)\}$, where the boundary points are equally spaced and the interior points are randomly chosen. Since the reason for the $\sqrt{\epsilon_{mach}}$ accuracy problem is the quadratic nature of $\sigma_1(\lambda)$ close to an eigenvalue λ_k and not the accuracy of the quadrature rule this simple approximation is justified. The smallest generalized singular value $\sigma_1(\lambda)$ is computed by the GSVD of $\{A_B(\lambda), A_I(\lambda)\}$. In the left plot of Figure 2.3 the function $\mu_1(\lambda)$ has a plateau of width in the order of $\sqrt{\epsilon_{mach}}$ close to λ_1 in which the values are essentially determined by numerical errors, making it hard to detect the minimum to more than the square root of machine precision. In contrast in the right plot of Figure 2.3 we show the computed value $\sigma_1(\lambda)$ on a finer scale. The function behaves almost linearly and the minimum can easily be determined to 12 digits and more (in [7] we give 14 digits).

Another attempt to solve this problem is to compute the zeros of the derivative $\mu_1'(\lambda)$ of $\mu_1(\lambda)$ instead of the minima of $\mu(\lambda)$. Such an approach was used by Driscoll with great success in a related method [12]. But this approach makes it necessary to accurately compute derivatives of $F(\lambda)$ and $G(\lambda)$, which might not always be possible.

3. The effect of ill-conditioning. The SVD approach of the MPS fails if the matrix $A_B(\lambda)$ is highly ill-conditioned for some λ far away from an eigenvalue since the MPS then approximates functions which are zero everywhere in the region. This cannot happen with the GSVD approach since we scale the approximate eigenfunctions to have unit norm in the interior of the region. But while the singular values of a matrix A are perfectly conditioned, the generalized singular values of a pencil $\{A, B\}$ might be ill-conditioned, introducing large errors in the computed generalized singular values. In this section we investigate these errors and their influence on the

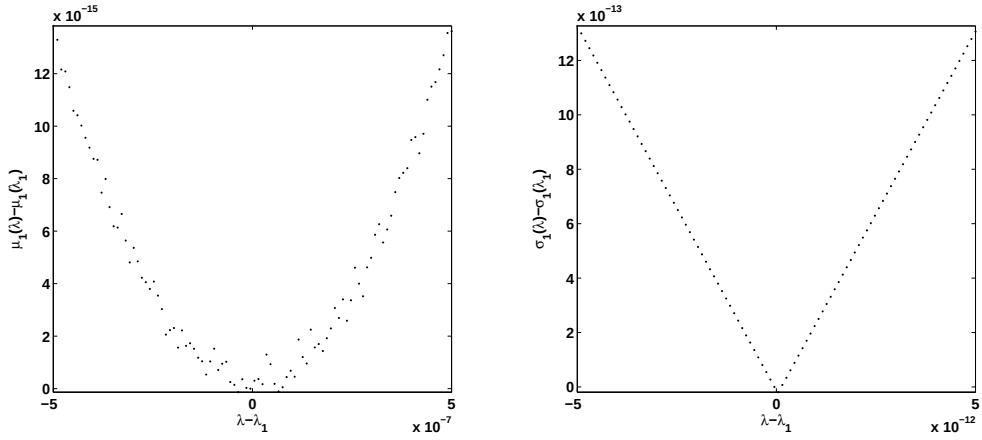

FIG. 2.3. *Left plot: The computed value* $\mu_1(\lambda) - \mu_1(\lambda_1)$ *close to* λ_1 *on the L-shaped region. Right plot: The value* $\sigma_1(\lambda) - \sigma_1(\lambda_1)$ *on the same region.*

ability to detect eigenvalues with the GSVD approach.

In Figure 3.1 we show the famous GWW-1 isospectral drum [13, 18]. Eigenfunctions on this region can have singularities at the four corners which are marked by black dots. To obtain accurate eigenvalue and eigenfunction approximations we need to represent these singularities in the approximation basis. With 60 basis functions around each singularity we obtain the approximation $\lambda_1 \approx 2.53794399979$ for the first eigenvalue on this region (for details see [7]). We believe all digits to be correct. Let us have a look at the corresponding plot of $\tan\theta(\lambda)$ in Figure 3.2 which is computed with Matlab's GSVD function as the smallest generalized singular value of the pencil $\{A_B(\lambda), A_I(\lambda)\}$. On the boundary we used 120 Chebyshev distributed points on each line segment and in the interior we spread 200 randomly distributed points in the smallest rectangle that contains the isospectral drum and then used those 88 points that were inside the drum. The values for different λ show a large variation before coming close to the first eigenvalue where the variation seems to disappear on this plotting scale. The matrix $A(\lambda) = \left[A_B(\lambda)^T A_I(\lambda)^T\right]^T$ is numerically almost singular for all values $\lambda > 0$.[2] But still we are able to detect the minimum of the subspace angle curve. In the following section we investigate this behavior in more detail.

3.1. The error of the GSVD. Let $A \in \mathbb{R}^{n\times p}$ and $B \in \mathbb{R}^{m\times p}$, $Y = \begin{bmatrix} A \\ B \end{bmatrix}$ and assume that $\operatorname{rank}(Y) = p$. We define a perturbed pencil $\{\tilde{A}, \tilde{B}\}$ as $\tilde{A} = A + \Delta A$ and $\tilde{B} = B + \Delta B$. If (s, c) is a generalized singular value pair of $\{A, B\}$, the corresponding perturbed generalized singular value pair of $\{\tilde{A}, \tilde{B}\}$ is denoted by $(\tilde{s}, \tilde{c})$. Furthermore, let $\sigma = \frac{s}{c}$ and $\tilde{\sigma} = \frac{\tilde{s}}{\tilde{c}}$ be the corresponding generalized singular values. The right generalized singular vector associated with σ is denoted by x and the right generalized singular vector associated with $\tilde{\sigma}$ is denoted by $\tilde{x}$. From Theorem 2.1 it follows that $\|Ax\|_2 = s$ and $\|Bx\|_2 = c$ with corresponding identities for the perturbed quantities.

The difference of $\tilde{\sigma}$ and σ can be estimated by considering condition numbers of

[2] We always scale the columns of $A(\lambda)$ to unit norm in order to avoid artifical ill-conditioning which is just due to the bad scaling of the Fourier-Bessel functions.

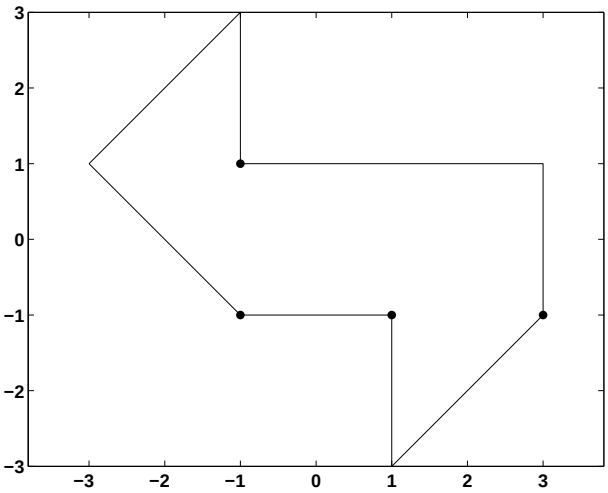

FIG. 3.1. *The famous GWW-1 isospectral drum. Eigenfunctions can only have singularities at the dotted corners.*

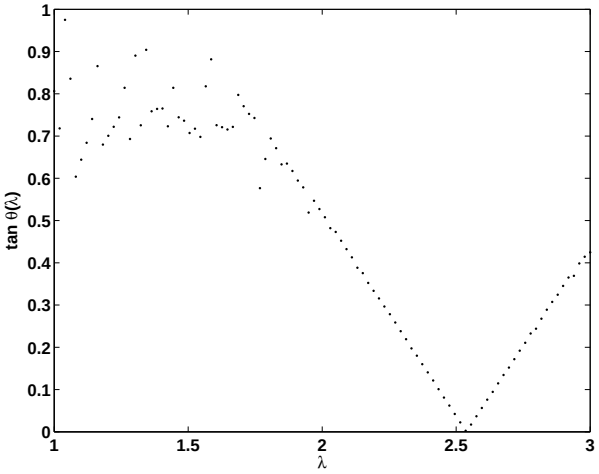

FIG. 3.2. *Plot of* $\tan\theta_1(\lambda)$ *for the GWW-1 isospectral drum. Before coming close to the first eigenvalue we can observe large variation.*

generalized singular values. Define

$$\mathrm{cond}(\sigma) = \lim_{\delta\to 0} \sup_{\max(\|E\|_2,\|F\|_2)\leq\delta} \frac{|\tilde{\sigma}-\sigma|}{\delta}.$$

In [26] Sun showed that for a simple, finite generalized singular value σ the condition number $\mathrm{cond}(\sigma)$ is

$$\mathrm{cond}(\sigma) = \frac{\|x\|_2(\|Ax\|_2+\|Bx\|_2)}{\|Bx\|_2^2} = \frac{\|x\|_2}{\|Bx\|_2}(1+\sigma) = \frac{\|x\|_2}{c}(1+\sigma). \tag{3.1}$$

The forward error of the GSVD is given as [26, eq. (2.3)]

$$|\tilde{\sigma}-\sigma| \leq \mathrm{cond}(\sigma)\max(\|\Delta A\|_2,\|\Delta B\|_2) + O\left(\max(\|\Delta A\|_2,\|\Delta B\|_2)^2\right). \tag{3.2}$$

Let us now return to the GSVD based MPS. In order for the GSVD approach to be successful we need to ensure that the perturbed value $\tilde{\sigma}_1(\lambda)$ is only small if λ is close to an eigenvalue λ_k. In [14] it is shown that

$$\frac{|\lambda - \lambda_k|}{\lambda_k} \leq C \min_{\Phi \in \mathcal{A}(\lambda)\setminus\{0\}} \frac{\|\Phi\|_{\partial\Omega}}{\|\Phi\|_{\Omega}} \tag{3.3}$$

for a constant $C > 0$ that only depends on the region. If we choose a sufficient number of well distributed boundary and interior points for the method then we can assume that

$$\frac{\|\Phi\|_{\partial\Omega}}{\|\Phi\|_{\Omega}} \approx \tilde{C} \frac{\|A_B(\lambda)x\|_{\partial\Omega}}{\|A_I(\lambda)x\|_{\Omega}}$$

for the vector x of coefficients of u in the basis particular solutions and a constant $\tilde{C} > 0$. A precise relationship between these quantities can be established by the use of quadrature rules and estimating their error. We obtain

$$\frac{|\lambda - \lambda_k|}{\lambda_k} \lesssim \hat{C} \min_{x \in \mathbb{R}^p \setminus \{0\}} \frac{\|A_B(\lambda)x\|_{\partial\Omega}}{\|A_I(\lambda)x\|_{\Omega}} = \hat{C}\sigma_1(\lambda) \tag{3.4}$$

for a constant $\hat{C}$. Numerical experiments in [8] suggest that this is indeed a good estimate. Hence, the unperturbed generalized singular value $\sigma_1(\lambda)$ cannot be small if λ is not close to λ_k and if we choose a sufficient number of discretization points.

In practice we are working with the perturbed generalized singular value $\tilde{\sigma}_1(\lambda)$ of the pencil $\{A_B(\lambda) + \Delta A_B(\lambda), A_I(\lambda) + \Delta A_I(\lambda)\}$. For a backward stable GSVD method we can assume that $\max\{\|\Delta A_B(\lambda)\|_2, \|\Delta A_I(\lambda)\|_2\} \leq K\epsilon_{mach}$, where K is a moderate constant that only depends on the dimension of the problem. Hence, from (3.2) it follows to first order that

$$|\tilde{\sigma}_1(\lambda) - \sigma_1(\lambda)| \leq K \frac{\|x_1(\lambda)\|_2}{c_1(\lambda)}(1 + \sigma_1(\lambda))\epsilon_{mach}. \tag{3.5}$$

Therefore, if $\|x_1(\lambda)\|_2$ is of moderate size, then we can expect that the errors in $\tilde{\sigma}_1(\lambda)$ are small. The following Lemma gives an estimate on $x_1(\lambda)$ depending on λ.

LEMMA 3.1. *Let $\sigma = s/c$ be a generalized singular value of the pencil $\{A, B\}$ and let x be its corresponding right generalized singular vector. Then*

$$\|x\|_2 \leq \frac{s}{\xi_p}, \tag{3.6}$$

where ξ_p is the smallest singular value of A.

Proof. From Theorem 2.1 we have $\|Ax\|_2 = s$. Since $\|Ax\|_2 \geq \xi_p\|x\|_2$ the result follows. □

Combining this Lemma with (3.5) leads to first order in ϵ_{mach} to

$$|\tilde{\sigma}_1(\lambda) - \sigma_1(\lambda)| \leq K \frac{\sigma_1(\lambda)}{\xi_p(\lambda)}(1 + \sigma_1(\lambda))\epsilon_{mach}, \tag{3.7}$$

where $\xi_p(\lambda)$ is the smallest singular value of $A_B(\lambda)$. Assume that

$$\tilde{\xi}_p(\lambda) \geq (1 + \tilde{\sigma}_1(\lambda))\epsilon_{mach} \tag{3.8}$$

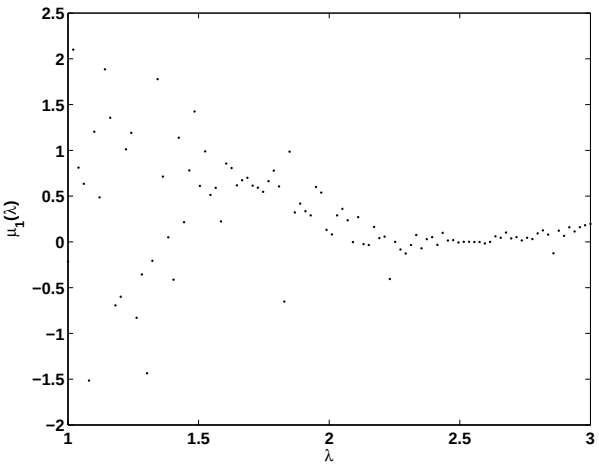

FIG. 4.1. $\mu_1(\lambda)$ *in the case of the GWW-1 isospectral drum.*

for the smallest singular value $\tilde{\xi}_p(\lambda)$ of $A_B(\lambda)+\Delta A_B(\lambda)$. Then if we treat $\{A_B(\lambda), A_I(\lambda)\}$ as a perturbation of $\{A_B(\lambda)+\Delta A_B(\lambda), A_I(\lambda)+\Delta A_I(\lambda)\}$ we obtain from (3.7) to first order the bound

$$|\tilde{\sigma}_1(\lambda) - \sigma_1(\lambda)| \leq K\tilde{\sigma}_1(\lambda).$$

Together with (3.4) it follows that

$$\frac{|\lambda - \lambda_k|}{\lambda_k} \lesssim \hat{C}(1+K)\tilde{\sigma}_1(\lambda). \tag{3.9}$$

Hence, even if we perturb $A_B(\lambda)$ and $A_I(\lambda)$, under the assumption that (3.8) holds we have a bound on the relative distance to the next eigenvalue which also implies that $\tilde{\sigma}_1(\lambda)$ can only become small close to an eigenvalue. But (3.8) is likely to hold for $\|\Delta A_B(\lambda)\|_2 \approx \epsilon_{mach}$. since then $\xi_p(\lambda)$ is perturbed by a quantity in the order of ϵ_{mach}.

4. Regularizing the GSVD. In practice it is often useful to remove the oscillations in the computed values for $\tan\theta_1(\lambda)$. Hence, we want to regularize the GSVD approach. In this section we will discuss a regularization strategy that is based on an idea by Barnett to regularize the generalized eigenvalue formulation.

Let us plot the smallest generalized eigenvalue $\mu_1(\lambda)$ of

$$A_B(\lambda)^T A_B(\lambda)x(\lambda) = \mu(\lambda)A_I(\lambda)^T A_I(\lambda)x(\lambda),$$

which is obtained by setting all weights to 1 in the quadrature rule used for the GEVD approach (see (2.8)). The resulting curve in Figure 4.1 shows large variation. Several of the computed values are negative and Matlab even returned some complex values for $\mu_1(\lambda)$. The problem is the large common numerical nullspace of $A_B(\lambda)$ and $A_I(\lambda)$. In [1] Barnett projected out this nullspace. Using our notation this can be done in the following way. Let

$$A_I(\lambda) = U(\lambda)\Sigma(\lambda)V(\lambda)^T$$

be the singular value decomposition of $A_I(\lambda)$. Now define a threshold $\hat{\epsilon}$ and let $\eta_1(\lambda) \geq \cdots \geq \eta_k(\lambda) > \hat{\epsilon}$ be the singular values of $A_I(\lambda)$ that are larger than $\hat{\epsilon}$. Partition $V(\lambda)$ as $V(\lambda) = [V_1(\lambda)\ V_2(\lambda)]$, where $V_1(\lambda)$ contains the first k columns and $V_2(\lambda)$ contains the last $p-k$ columns of $V(\lambda)$. Then the regularized generalized eigenvalue problem is defined as

$$V_1(\lambda)^T A_B(\lambda)^T A_B(\lambda) V_1(\lambda)\hat{x}(\lambda) = \hat{\mu}(\lambda) V_1(\lambda)^T A_I(\lambda)^T A_I(\lambda) V_1(\lambda)\hat{x}(\lambda).$$

A similar strategy was proposed and analyzed by Fix and Heiberger in [16]. The right-hand side matrix now has the singular values $\eta_1(\lambda)^2 \geq \cdots \geq \eta_k(\lambda)^2 > \hat{\epsilon}^2$. Therefore, to remove all numerically zero singular values of $A_I(\lambda)^T A_I(\lambda)$ we need to chose $\hat{\epsilon} > \sqrt{\epsilon_{mach}}$. In [1] Barnett uses a threshold of $\hat{\epsilon} = 10^{-7}$.

We can apply the same strategy to the GSVD formulation. Then instead of finding the smallest generalized singular value $\sigma_1(\lambda)$ of the pencil $\{A_B(\lambda), A_I(\lambda)\}$ we find the smallest generalized singular value $\hat{\sigma}_1(\lambda)$ of $\{A_B(\lambda)V_1(\lambda), A_I(\lambda)V_1(\lambda)\}$.

But for the GSVD the following strategy to obtain a regularization matrix $V_1(\lambda)$ is more suitable. Let

$$\begin{bmatrix} A_B(\lambda) \\ A_I(\lambda) \end{bmatrix} = \begin{bmatrix} Q_B(\lambda) \\ Q_I(\lambda) \end{bmatrix} R(\lambda)$$

be the QR decomposition of $A(\lambda)$. Compute the SVD of $R(\lambda)$ as

$$R(\lambda) = U_R(\lambda)\Sigma_R(\lambda)V_R(\lambda)^T. \tag{4.1}$$

Note that the singular values of $R(\lambda)$ are identical to those of $\begin{bmatrix} A_B(\lambda)^T & A_I(\lambda)^T \end{bmatrix}^T$. The regularization matrix $V_1(\lambda)$ is defined as the first k columns of $V_R(\lambda)$ associated with those singular values of $R(\lambda)$ which are above the threshold $\hat{\epsilon}$. The generalized singular values of $\{A_B(\lambda)V_1(\lambda), A_I(\lambda)V_1(\lambda)\}$ are now identical to those of $\{Q_B(\lambda)U_1(\lambda), Q_I(\lambda)U_1(\lambda)\}$, where $U_1(\lambda)$ contains the first k columns of $U_R(\lambda)$. The smallest generalized singular value of $\{A_B(\lambda), A_I(\lambda)\}$ is only modestly changed with this strategy if it is not too ill-conditioned. This is shown in the following theorem.

THEOREM 4.1. *Let $\sigma_1 = s_1/c_1$ be the smallest generalized singular value and x_1 its corresponding right generalized singular vector of the pencil $\{A, B\}$ with $A \in \mathbb{R}^{n\times p}$ and $B \in \mathbb{R}^{m\times p}$. Let the regularization matrix $V_1 \in \mathbb{R}^{p\times k}$ be obtained by the strategy described above and denote by $\hat{\sigma}_j$ $j = 1, \ldots, k$ the generalized singular values of the pencil $\{AV_1, BV_1\}$. Then*

a) For all generalized singular values $\hat{\sigma}_j$ of the pencil $\{AV_1, BV_1\}$,

$$\sigma_j \leq \hat{\sigma}_j.$$

b) If $\hat{\epsilon}\|x_1\|_2 < c_1$, then

$$\sigma_1 \leq \hat{\sigma}_1 \leq \frac{s_1 + \hat{\epsilon}\|x_1\|_2}{c_1 - \hat{\epsilon}\|x_1\|_2}.$$

Proof. Let V_2 be the orthogonal complement of V_1, i.e. $V = [V_1\ V_2]$ is an orthogonal matrix. Then $\|AV_2y\|_2 \leq \hat{\epsilon}\|y\|_2$ and $\|BV_2y\|_2 \leq \hat{\epsilon}\|y\|_2$ for all $y \in \mathbb{R}^{p-k}$ since $\| \begin{bmatrix} AV_2 \\ BV_2 \end{bmatrix} \|_2 \leq \hat{\epsilon}$. Let $x_1 = V_1y_1 + V_2y_2$. We have

$$\|AV_1y_1\|_2 = \|Ax_1 - AV_2y_2\|_2 \leq \|Ax_1\|_2 + \|AV_2y_2\|_2 \leq s_1 + \hat{\epsilon}\|y_2\|_2$$

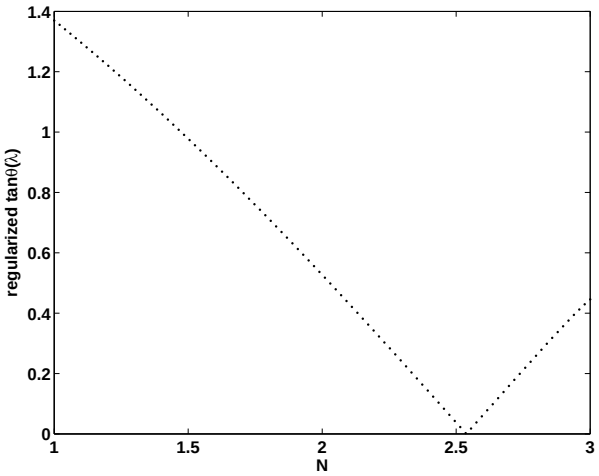

FIG. 4.2. *The regularized curve of* $\tan\theta_1(\lambda)$ *for the GWW-1 isospectral drum. The variation has disappeared on this plotting scale (compare with Figure 3.2).*

and

$$\|BV_1y_1\|_2 = \|Bx_1 - BV_2y_2\|_2 \geq \|Bx_1\|_2 - \|BV_2y_2\|_2 \geq c_1 - \hat{\epsilon}\|y_2\|_2.$$

With $\|y_2\|_2 \leq \|x_1\|_2$ and the minimax characterization in (2.4) it follows that

$$\hat{\sigma}_1 \leq \frac{\|AV_1y_1\|_2}{\|BV_1y_1\|_2} \leq \frac{s_1 + \hat{\epsilon}\|x_1\|_2}{c_1 - \hat{\epsilon}\|x_1\|_2}.$$

The fact that $\sigma_j \leq \hat{\sigma}_j$ $j = 1, \ldots, k$ also follows immediately from (2.4) since restricting the pencil $\{A, B\}$ to $\{AV_1, BV_1\}$ corresponds to minimizing only over a subset of all possible subspaces. □

A similar result for the regularization of ill-conditioned generalized eigenvalue problems was proved in [16]. Let us apply this theorem to the pencil $\{A_B(\lambda), A_I(\lambda)\}$. If $\sigma_1(\lambda) \ll 1$ close to an eigenvalue then $c_1(\lambda) \approx 1$ and we obtain

$$\begin{aligned}\hat{\sigma}_1(\lambda) &\leq \frac{s_1(\lambda) + \hat{\epsilon}\|x_1(\lambda)\|_2}{c_1(\lambda) - \hat{\epsilon}\|x_1(\lambda)\|_2} \approx \frac{\sigma(\lambda) + \hat{\epsilon}\|x_1(\lambda)\|_2}{1 - \hat{\epsilon}\|x_1(\lambda)\|_2} \\ &= \sigma_1(\lambda) + (1 + \sigma_1(\lambda))\hat{\epsilon}\|x_1(\lambda)\|_2 + O((\hat{\epsilon}\|x_1(\lambda)\|_2)^2).\end{aligned}$$

Hence, to first order the change of $\sigma_1(\lambda)$ is essentially at most $\hat{\epsilon}\|x_1(\lambda)\|_2$. This result can also be obtained by noting that $\|A_B(\lambda) - A_B(\lambda)V_1(\lambda)V_1(\lambda)^T\|_2 \leq \hat{\epsilon}$, $\|A_I(\lambda) - A_I(\lambda)V_1(\lambda)V_1(\lambda)^T\|_2 \leq \hat{\epsilon}$ and applying (3.2).

Therefore, close to an eigenvalue we can expect only a small penalty due to this regularization strategy if $\|x_1(\lambda)\|_2$ is of moderate size there. For example in the case of the GWW-1 isospectral drum the parameter $\hat{\epsilon} = 10^{-14}$ leads to $\hat{\sigma}_1(\lambda_1) = 2.3 \times 10^{-11}$, while the original value is $\sigma_1(\lambda_1) = 1.90 \times 10^{-11}$. The upper bound from Theorem 4.1 is $\hat{\sigma}_1(\lambda_1) \leq 7.76 \times 10^{-11}$. The right generalized singular vector $x_1(\lambda_1)$ has a magnitude of 10^3 in that example. In Figure 4.2 the regularized curve $\tan\hat{\theta}_1(\lambda) = \hat{\sigma}_1(\lambda)$ is plotted. The variation away from the eigenvalue is not visible on this scale any more. The following argument due to Eisenstat explains this effect.

Let $\hat{\epsilon}$ be the regularization parameter, let $y(\lambda)$, $\|y(\lambda)\|_2 = 1$ be a right singular vector corresponding to the smallest singular value $\xi_p(\lambda)$ of $A_B(\lambda)V_1(\lambda)$, and let $\psi_p(\lambda) = \|A_I(\lambda)V_1(\lambda)y(\lambda)\|_2$. Then by definition

$$\xi_p(\lambda)^2 + \psi_p(\lambda)^2 = \left\| \begin{bmatrix} A_B(\lambda) \\ A_I(\lambda) \end{bmatrix} V_1(\lambda)y(\lambda) \right\|_2^2 \geq \hat{\epsilon}^2$$

and $\hat{\sigma}_1(\lambda) \leq \frac{\xi_p(\lambda)}{\psi_p(\lambda)}$. Ignoring the higher order term and the factor $1 + \sigma_1(\lambda)$ in (3.7), the computed value $\tilde{\sigma}_1(\lambda)$ from the regularized problem satisfies

$$|\tilde{\sigma}_1(\lambda) - \hat{\sigma}_1(\lambda)| \leq \hat{\sigma}_1(\lambda) K \frac{\epsilon_{mach}}{\xi_p(\lambda)}.$$

If $\xi_p(\lambda) \geq \frac{\hat{\epsilon}}{\sqrt{2}}$, then

$$|\tilde{\sigma}_1(\lambda) - \hat{\sigma}_1(\lambda)| \leq \sqrt{2}\hat{\sigma}_1(\lambda) \frac{K\epsilon_{mach}}{\hat{\epsilon}},$$

which is a relative bound if $\hat{\epsilon} > \sqrt{2}K\epsilon_{mach}$; If $\xi_p(\lambda) < \frac{\hat{\epsilon}}{\sqrt{2}}$ then $\psi_p(\lambda) \geq \frac{\hat{\epsilon}}{\sqrt{2}}$. Together with $\hat{\sigma}_1(\lambda) \leq \frac{\xi_p(\lambda)}{\psi_p(\lambda)}$ it follows that

$$|\tilde{\sigma}_1(\lambda) - \hat{\sigma}_1(\lambda)| \leq K \frac{\epsilon_{mach}}{\psi_p(\lambda)} \leq \sqrt{2}K \frac{\epsilon_{mach}}{\hat{\epsilon}},$$

an absolute bound. By increasing $\hat{\epsilon}$ we reduce the bound on the difference between the computed and the exact smallest generalized singular value of the regularized problem in both cases.

The SVD based regularization strategy proposed in this section is not the only possible strategy. One can also apply a rank-revealing QR decomposition to $\begin{bmatrix} A_B(\lambda) \\ A_I(\lambda) \end{bmatrix}$ that selects a subset of the columns of this matrix and thereby avoids round-off errors introduced by multiplying $Q_B(\lambda)U_1(\lambda)$. In practice both strategies behaved similarly for our examples.

5. Limits of the GSVD approach. What are the limits of the GSVD approach? Assume that we have a basis of particular solutions for which

$$\min_{\Phi \in \mathcal{A}(\lambda_k)} \frac{\|\Phi\|_{\partial\Omega}}{\|\Phi\|_\Omega} = O(\epsilon_{mach}), \tag{5.1}$$

where λ_k is an eigenvalue of (1.1). Hence, with a good discretization it also follows that $\sigma_1(\lambda_k) = O(\epsilon_{mach})$.

Then it is still possible that the coefficient vector $c = (c_1, \ldots, c_p)^T$ of the function

$$\Phi = \sum_{k=1}^{p} c_k \Phi_k$$

from $\mathcal{A}(\lambda)$ that achieves the minimum in (5.1) has very large coefficients, that is $\|c\|_2 \gg 1$.

But then we can also expect that $\|x_1(\lambda_k)\|_2 \gg 1$, where $x_1(\lambda_k)$ is the right generalized singular vector associated with the generalized singular value $\sigma_1(\lambda_k)$.

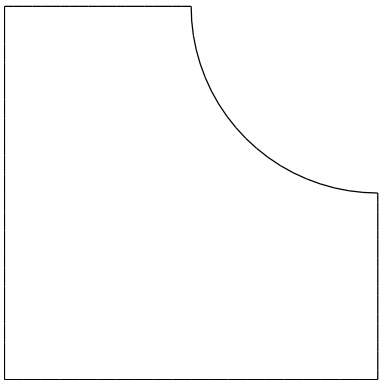

FIG. 5.1. *A circular L region*

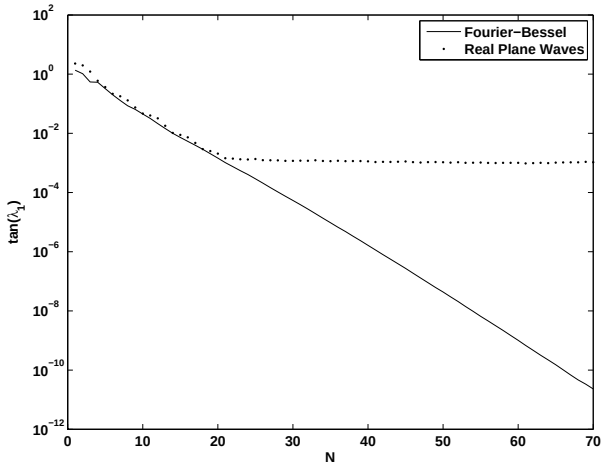

FIG. 5.2. *Convergence of* $\sigma_1(\lambda_1) = \tan\theta_1(\lambda_1)$ *on the circular L region using a Fourier-Bessel and a real plane wave basis set.*

This may limit the accuracy to which we can compute $\sigma_1(\lambda_k)$ in floating point arithmetic. From (3.5) it follows that to first order

$$|\tilde{\sigma}_1(\lambda) - \sigma_1(\lambda)| \leq K\frac{\|x_1(\lambda)\|_2}{c_1(\lambda)}(1+\sigma_1(\lambda))\epsilon_{mach} \approx K\|x_1(\lambda)\|_2\epsilon_{mach}$$

for $\sigma_1(\lambda) \ll 1$. We therefore have to expect in the worst case that $\tilde{\sigma}_1(\lambda_k) \approx \sigma_1(\lambda_k) + K\|x_1(\lambda_k)\|_2\epsilon_{mach} \gg \sigma_1(\lambda_k)$.

This shows that it is not enough to have a basis of particular solutions that can approximate an eigenfunction to high accuracy. We also need to ensure that the coefficients of the approximate eigenfunction in that basis do not grow too much.

Figure 5.2 shows $\sigma_1(\lambda_1) = \tan\theta_1(\lambda_1)$ for two different basis sets at the smallest eigenvalue λ_1 of the circular L region in Figure 5.1. Using a growing number of Fourier-Bessel functions we can minimize $\sigma_1(\lambda_1)$ until 10^{-12}. But with a real plane wave basis that theoretically leads to the same rate of convergence on this region we can minimize $\sigma_1(\lambda)$ only up to 10^{-3}. This becomes clear by looking at $\|x_1(\lambda_1)\|_2$.

If $N = 20$ we have for the Fourier-Bessel basis the value $\|x_1(\lambda_1)\|_2 \approx 10$, while

the same value for the real plane wave basis is approximately 9.7×10^{12}. One might be tempted to explain this effect purely algebraically with the condition numbers of the discrete basis $A(\lambda_1) = \begin{bmatrix} A_B(\lambda_1) \\ A_I(\lambda_1) \end{bmatrix}$. At $N = 20$ for the Fourier-Bessel basis set we have $\kappa_2(A(\lambda_1)) \approx 3.8 \times 10^3$ and for the plane waves we obtain the value 9.7×10^{14}, where $\kappa_2(A(\lambda_1))$ is the condition number in the 2-norm of $A(\lambda_1)$. However, at $N = 70$ the condition number of the Fourier-Bessel basis set has grown to $\kappa_2(A(\lambda_1)) \approx 9 \times 10^{13}$. But still we only have $\|x_1(\lambda_1)\|_2 \approx 2.8 \times 10^3$ for this basis set.

This behavior cannot be improved by regularization since it follows from Theorem 4.1 that the error in $\sigma_1(\lambda)$ introduced by regularizing is itself in the order of $\hat{\epsilon}\|x_1(\lambda)\|_2$.

We emphasize that the coefficient growth phenomenon is not a property of a certain algorithm to find approximate eigenfunctions of a set of particular solutions but a property of the underlying basis set itself. For fundamental solution bases this was recently investigated in [3].

6. Conclusions. In this article we showed that the GSVD is the right framework to compute accurate approximations of eigenvalues and eigenfunctions of (1.1) from a basis of particular solutions. While SVD-based approaches fail if $A_B(\lambda)$ is highly ill-conditioned, the GSVD still allows accurate approximations of eigenvalues and eigenfunctions in this case as the two examples suggest. Eigenvalues and eigenfunctions on several challenging regions are also computed in [6, 7, 27] with the subspace angle method which is equivalent to the GSVD approach as we showed in Section 2.2. The advantage compared to the GEVD is that we do not work with a squared formulation that may suffer from limited accuracy. Furthermore, the regularization strategy discussed in Section 4 allows us to smooth the curve $\sigma_1(\lambda)$ with only a small penalty on the minimum of the curve at an eigenvalue λ_k. Accurate bounds for the relative distance of an approximation λ to the next eigenvalue λ_k can also be obtained from the smallest generalized singular value $\sigma_1(\lambda)$. This is discussed in [7, 8, 14].

The choice of optimal sets of particular solutions for different regions is currently under investigation. But if the basis admits approximations to high accuracy then as this paper shows the GSVD approach is a robust and easily implementable way to obtain them.

Acknowledgements. Most of this work was done as a D.Phil student of Nick Trefethen at Oxford University. His comments and ideas were invaluable for this work. I am also very grateful for the discussions with Stan Eisenstat. His remarks significantly improved this paper. Alex Barnett pointed me to the work done by physicists on this subject and also contributed many fruitful suggestions. I would also like to thank Heike Fassbender and Jens Zemke for their comments on the first drafts of this paper.

REFERENCES

[1] A. H. Barnett, *Dissipation in deforming chaotic billiards*, Ph.D thesis, Department of Physics, Harvard University, 2000.

[2] A. H. Barnett, *Inclusion of Dirichlet eigenvalues in the semiclassical limit via a boundary spectral problem*, in preparation.

[3] A. H. Barnett and T. Betcke, *Stability and convergence of the method of fundamental solutions for Helmholtz problems on analytic domains*, submitted to J. Comp. Phys.

[4] S. Bergman, *Über ein Verfahren zur Konstruktion der Näherungslösungen der Gleichung* $\Delta u + \tau^2 u = 0$. *Anhang zur Arbeit: Über die Knickung von rechteckigen Platten bei Schubbeanspruchung.*, Appl. Math. Mech. 3 (1936), pp. 97–106.

[5] M. V. Berry, *Evanescent and real waves in quantum billiards and Gaussian beams*, J. Phys. A, 27 (1994), pp. L391–L398.
[6] T. Betcke and L. N. Trefethen, *Computations of eigenvalue avoidance in planar domains*, Proc. Appl. Math. Mech., 4 (2004), pp. 634–635.
[7] T. Betcke and L. N. Trefethen, *Reviving the method of particular solutions*, SIAM Rev., 47 (2005), pp. 469–491.
[8] T. Betcke, *Numerical computation of eigenfunctions of planar regions*, D.Phil thesis, Computing Laboratory, Oxford University, 2005.
[9] A. Bogomolny, *Fundamental solutions method for elliptic boundary value problems*, SIAM J. Numer. Anal., 22 (1985), pp. 644–669.
[10] H. D. Conway and K. A. Farnham, *The free flexural vibrations of triangular, rhombic and parallelogram plates and some analogies*, Int. J. Mech. Sci., 7 (1965), pp. 811–816.
[11] H. D. Conway and A. W. Leissa, *A method for investigating certain eigenvalue problems of the buckling and vibration of plates*, J. Appl. Mech., 27 (1960), pp. 557–558.
[12] J. Descloux and M. Tolley, *An accurate algorithm for computing the eigenvalues of a polygonal membrane*, Comput. Methods Appl. Mech. Engrg., 39 (1983), pp. 37–53.
[13] T. A. Driscoll, *Eigenmodes of isospectral drums*, SIAM Rev., 39 (1997), pp. 1–17.
[14] S. C. Eisenstat, *On the rate of convergence of the Bergman-Vekua method for the numerical solution of elliptic boundary value problems*, SIAM J. Numer. Anal., 11 (1974), pp. 654–680.
[15] R. Ennenbach and H. Niemeyer, *The inclusion of Dirichlet eigenvalues with singularity functions*, Z. Angew. Math. Mech. 76 (1996), pp. 377–383.
[16] G. Fix and R. Heiberger, *An algorithm for the ill-conditioned generalized eigenvalue problem*, SIAM J. Numer. Anal., 9 (1972), pp. 78–88.
[17] L. Fox, P. Henrici, and C. B. Moler, *Approximations and bounds for eigenvalues of elliptic operators*, SIAM J. Numer. Anal., 4 (1967), pp. 89–102.
[18] C. Gordon, G. Webb, and S. Wolpert, *Isospectral plane domains and surfaces via Riemannian orbifolds*, Invent. Math., 110 (1992), pp. 1–22.
[19] E. J. Heller, *Bound-state eigenfunctions of classically chaotic Hamiltonian systems: Scars of periodic orbits*, Phys. Rev. Lett., 53 (1984), pp. 1515–1518.
[20] E. J. Heller, *Wavepacket dynamics and quantum chaology*, In M. J. Giannoni, A. Voros, and J. Zinn-Justin, editors, *Proceedings of the 1989 Les Houches summer school on "Chaos and Quantum Physics"*, pp. 547–663, North Holland, 1991. Elsevier Science Publishers B. V.
[21] J. R. Kuttler and V. G. Sigillito, *Bounding eigenvalues of elliptic operators*, SIAM J. Math. Anal., 9 (1978), pp. 768–773.
[22] S. R. Kuo and W. Yeih and Y. C. Wu, *Applications of the generalized singular-value decomposition method on the eigenproblem using the incomplete boundary element formulation*, Journal of Sound and Vibration 235 (2000), pp. 813–845.
[23] R. Mathon and R. L. Johnston, *The approximate solution of elliptic boundary-value problems by fundamental solutions*, SIAM J. Numer. Anal. 14 (1977), pp. 638–650.
[24] C. B. Moler, *Accurate bounds for the eigenvalues of the Laplacian and applications to rhombical domains*, Report CS-TR-69-121 (1969), Department of Computer Science, Stanford University, available at `ftp://reports.stanford.edu/pub/cstr/reports/cs/tr/69/121/CS-TR-69-121.pdf`
[25] C. C. Paige and M. A. Saunders, *Towards a generalized singular value decomposition*, SIAM J. Numer. Anal., 18 (1981), pp. 398–405.
[26] J. G. Sun, *Condition number and backward error for the generalized singular value decomposition*, SIAM J. Matrix Anal. Appl., 22 (2000), pp. 323–341.
[27] L. N. Trefethen and T. Betcke, *Computed eigenmodes of planar regions*, AMS Contemp. Math., 412 (2006), pp. 297–314.